Hu, X., Zang, A., Heidbach, O., Cui, X., Xie, F., Chen, J. (2017): Crustal stress pattern in China and its adjacent areas. - *Journal of Asian Earth Sciences*, *149*, pp. 20—28.

DOI: http://doi.org/10.1016/j.jseaes.2017.07.005

Crustal Stress Pattern in China and Its Adjacent Areas

Xingping Hu[a,b,*], Arno Zang[c], Oliver Heidbach[c], Xiaofeng Cui[b], Furen Xie[b], Jiawei Chen[b]
a School of Earth and Space Science, University of Science and Technology of China, 230026 Hefei, China
b Key Laboratory of Crustal Dynamics, Institute of Crustal Dynamics, China Earthquake Administration, 100085 Beijing, China
c GFZ German Research Centre for Geosciences, Telegrafenberg, 14473 Potsdam, Germany

** Corresponding author. Xingping Hu. School of Earth and Space Science, University of Science and Technology of China, 230026 Hefei, China*
Telephone: +8601062846726, +8613811111002
E-mail address: huxp1987@163.com (Xingping Hu).

Abstract

During the update of the World Stress Map (WSM) database, we integrated the China stress database by strictly using the internationally developed quality ranking scheme for each individual stress data record. This effort resulted in a comprehensive and reliable dataset for the crustal stress of China and its adjacent areas with almost double the amount of data records from the WSM database release 2008, i.e., a total of 8,228 data records with reliable A-C qualities in the region of 45-155° East and 0-60° North. We use this dataset for an analysis of the stress pattern for the orientation of maximum compressive horizontal stress (S_{Hmax}). In contrast to earlier findings that suggested that the mean S_{Hmax} orientation would be aligned with the direction of plate motion, we clearly see from our results that the plate boundary forces, as well as topography and faulting, are important control factors for the overall stress pattern. Furthermore, the smoothing results indicate that the S_{Hmax} orientation in China rotates clockwise from the west to the east, which results in a fan-shaped crustal stress pattern for the continental scale. The plate boundary forces around China, which are the Indian-Eurasian plate collision in the west and the Pacific plate subduction and the push from the Philippine plate in the east, can still be seen as the key driving processes and the first-order controls for the crustal stress pattern. The South-North seismic zone can be seen as the separation zone for the western and eastern plate boundary forces. Topographic variation and faulting activity, however, provide second-order changes, and lead to local variations and different inhomogeneity scales for the stress pattern. Due to differences in these factors, Northeast China and the central part of the Tibetan plateau have notably homogeneous stress patterns, while the South-North seismic zone, the Hindu Kush-Pamir region, and the Taiwan region have extremely inhomogeneous stress patterns. Furthermore, the different behaviors of stress orientations around continental and oceanic plate boundaries could imply that complicated mechanisms exist and warrant further and more specific studies.

Keywords: stress data integration; China and its adjacent areas; stress orientation; inhomogeneity scale; geodynamic interpretation

1. Introduction

The crustal stress state is a key parameter for our understanding of geodynamic processes, seismic hazard assessment and the stability of underground openings (Zang and Stephansson, 2010; Zoback, 2007; Fuchs and Müller, 2001). There are different stress indicators regarding the crustal stress state, such as earthquake focal mechanism solutions, borehole breakouts, hydraulic fracturing tests, overcoring, and geological data. However, obtaining complete information for the 3D stress field (i.e., the six independent components of the stress tensor) remains a challenging task (Schmitt et al., 2012; Stephansson and Zang, 2010). It is also complicated to display either a full or partial representation of the stress tensor in an easily interpretable manner (Lund and Townend, 2007). The orientation of the maximum horizontal stress S_{Hmax} determines the orientation of the 3D stress tensor when assuming that the vertical stress S_V, also called lithostatic overburden, is a principal stress. The pattern of the S_{Hmax} orientation, which is able to reflect the dynamic background (Zoback, 1992; Townend and Zoback, 2006, 2004), became a feasible representation for a stress field and was widely used for research in the stress field at a global scale (Heidbach et al., 2010, 2007; Sperner et al., 2003; Zoback, 1992; Zoback et al., 1989) as well as at regional and local scales (Rajabi et al., 2016; Xie et al., 2015, 2007; Reiter et al., 2014; Balfour et al., 2011; Reinecker et al., 2010; Rebaï et al., 2007; Brudy and Kjørholt, 2001; Hillis et al, 1998; Coblentz et al., 1998; Müller et al., 1997, 1992; Bird and Li, 1996; Sbar and Sykes, 1973).

The World Stress Map (WSM) project is a global compilation of information on the crustal stress field from a wide range of stress indicators. This systematic work of WSM began in 1986 as a Task Force of the International Lithosphere Program (ILP) under the leadership of Mary Lou Zoback, and WSM was a research project at the Heidelberg Academy of Sciences then. The WSM is a collaborative project that includes the input and expertise of many scientists worldwide, and it provides free information on its website located at www.world-stress-map.org. Since 2009, the WSM project has been maintained by the Helmholtz Center Potsdam - German Research Center for Geosciences GFZ. The amount of data records has increased from ~7700 in the first WSM database release 1992 to 21,750 in the WSM database release 2008 (Heidbach et al., 2010, 2009).

Complementary to the ongoing effort of stress data compilation within the WSM project, the research of stress field and stress data compilation was established in China (Cui et al., 2005; Xie et al., 2004; Xu et al., 2001, 1989; Wang et al., 1993, 1980; Yan et al., 1979; Deng and Zhang, 1979). Between 2000 and 2002, the Institute of Crustal Dynamics collected a wide variety of stress data in China, conducted comprehensive work on the crustal stress field of the Chinese continent, compiled the China stress map, and built the Fundamental Database of Crustal Stress Environment in Continental China (hereafter referred to as the China Stress Database). The China Stress Database is the first fundamental database that incorporates various stress data records (Xie et al., 2007). It has been updated continuously since 2002, and up to now, the number of data records inputted has exceeded 7000 entries. Based on these stress data, the latest version of the Recent Tectonic Stress Map of China and its Adjacent Areas has been published, which mainly represents the various stress data and also shows the achievements of stress division and stress trajectory for the stress field in China (Xie et al., 2015).

Both the WSM project and the stress field research in China have accumulated an abundance of stress data. However, the WSM database and the China Stress Database were never well integrated into each other to allow for a higher resolution of the stress pattern beyond the national borders. Therefore, during the course of the current global effort to publish the WSM database release 2016 (Heidbach et al, 2016) for the 30th anniversary of the WSM project, the collaboration between China and the WSM intensified in order to integrate the two databases into each other and conduct further investigations on the stress pattern in China and its adjacent areas.

This paper presents the integration of stress data from the WSM database and the latest China Stress Database. This effort not only resulted in a significant increase in the amount of data records but also led to a comprehensive dataset with a higher reliability and better resolution for the first time in two decades. This paper also presents an analysis of the stress pattern for the S_{Hmax} orientation by using two different smoothing schemes, in order to reveal regional and local variability of the stress pattern and its relationship with geodynamic processes and/or structural sources.

2. Brief tectonic stress background of China and its adjacent areas

China is located in the southeastern portion of the Eurasian plate, and it is an important part of the plate. There are four other plates around China: the Indian plate, the Pacific plate, the Philippine plate, and the North American plate. The influence from the North American plate is quite marginal for the tectonic deformation of China (Zhang et al., 2002). Therefore, the main plate boundary forces are from the Indian plate, the Pacific plate, and the Philippine plate (Fig. 1). The western force source is primarily generated by the Indian plate's northwestward collision with the Eurasian plate, while the eastern force source includes the combined effect of the Pacific plate subduction and the push from the Philippine plate. Among all the boundary forces, the influence of Indian-Eurasian collision was determined to be the largest according to some geodynamic simulations (Zhu et al., 2006; Wang et al., 1996). There are four key regions for the transmission of plate forces corresponding to the plate boundaries: the Himalayan west tectonic knot, the Himalayan east tectonic knot, the deep seismic area in Northeast China, and the Taiwan region. The former two regions are the tectonic knots of the Indian-Eurasian collision, and they are located in the Hindu Kush-Pamir region and the southeast margin of the Tibetan plateau, respectively. The Northeast China and the Taiwan Region are the key regions for the transmission of plate forces from the Pacific plate and from the Philippine plate. Due to the crucial tectonic locations, these four regions have been the focus regions for research of geodynamic processes as well as the tectonic stress field for several decades, and they also have a great significance for this study.

Under the control of the surrounding tectonism, the stress field in China and its adjacent areas shows obvious divisional features, which are manifested as different stress orientations, stress regimes, and stress intensities in different regions (Xie et al., 2015). By using different methods, such as focal mechanism analysis and numerical simulation, some scholars have investigated the crustal stress field for all of China and/or some regions in China. One significant feature that has been commonly found is that the S_{Hmax} orientations in China rotate clockwise from the west to the east (Xie et al., 2015, 2007, 2004; Fan et al., 2012; Cui et al., 2005; Xu et al., 2001, 1989; Wang et al., 1996, 1993, 1980; Yan et al., 1979; Deng and Zhang, 1979), but more details with a higher resolution will still contribute to an improved understanding of the stress field in China.

More reliable and various stress data could help to reveal a more comprehensive and refined stress pattern. Among the analysis methods for stress orientations, the smoothing algorithm (Heidbach et al., 2010; Zang and Stephansson, 2010; Müller et al. 2003; Hansen and Mount, 1990; Watson, 1985) provides a means of identifying significant patterns in sets of oriented data by eliminating local perturbations in the observations and by predicting patterns of oriented data in places which lack observations. Consequently, the smoothing algorithm is an effective mathematical way to analyze stress orientation characteristics. Therefore, a further study with more reliable stress data and an appropriate smoothing method could better describe the crustal stress pattern and its inhomogeneity. This would help to reveal more details of the crustal stress field and improve its geodynamic interpretation in China and its adjacent areas.

3. Integration of stress data in China and its adjacent areas

First, we integrated the latest China Stress Database (Xie et al., 2015) and the WSM database for more reliable stress data. The China Stress Database provides 6089 chosen data records with 3983 data records from earthquake focal mechanism solutions (FMSs), 454 data records from borehole breakouts and drilling induced tensile fractures, 544 geological fault slip data records, 459 hydraulic fracture data records and 649 overcoring data records. Some FMSs of small earthquakes and aftershocks, as well as a few unpublished stress measurement data, were not integrated. Due to differences in the quality assessment used for the China Stress Database and the WSM, each data record was referenced again, and the latest WSM quality ranking scheme from Heidbach et al. (2010) was applied. In these stress data, most of the overcoring data were stored as single individual measurements, and thus were not in agreement with the ranking requirements of the WSM. Therefore, we calculated the mean value for those overcoring measurements with the same location and from the same original reference, and received 203 overcoring data records at different locations. In total, 5643 stress data records from the China Stress Database were finally obtained and integrated into the WSM database release 2016 (Heidbach et al., 2016).

After removing the duplicated stress data, we obtained a comprehensive and reliable dataset for the crustal stress of China and its adjacent areas. In the region of 45-155° East and 0-60° North, there are 11,255 stress data records (Table 1) with A-E qualities, of which 8,228 have A-C qualities. Among these A-C quality stress data records, 1884 FMS data records with the criteria of a Possible Plate Boundary Event (PBE) were considered as PBEs (Heidbach et al., 2010, 2009, 2008; Townend, 2006).

This means that these FMS data have a larger potential for a large offset between the P-, B-, and T-axes and the principal stress orientations. Therefore, these 1884 FMS data records were removed, and the remaining 6344 stress data records (Fig. 2) were used to analyze the stress field in China and its adjacent areas for this study.

Through the data check and quality reassignment, the stress data qualities were evaluated and verified, and the A-C quality stress data records could be considered reliable for the analysis of the stress pattern and the interpretation of geodynamic processes. Compared with the previous WSM database release 2008 (Fig. 3a), the amount of the stress data has increased significantly (Fig. 3b) all over the region, which provides a good basis for further investigating the stress pattern in China and its adjacent areas.

According to the distribution of stress data in China and its adjacent areas as depicted in Fig. 2, it is evident that the stress data cover the majority of China, but with an inhomogeneous data distribution. Quite many data points assemble in some places, such as the east margin of the Tibetan plateau and the Hindu Kush-Pamir region, while only few data points distribute in some other parts, such as the Ordos basin, the Tarim basin, and the South China. The S_{Hmax} orientations have good consistency in some places, such as in Northeast China and the central part of the Tibetan Plateau, but the orientations scatter in some other places, such as in the east margin of the Tibetan Plateau. Another phenomenon that should be considered in the stress field analysis, is that some disperse orientation data points cluster in a very small place, or even at almost the same place, such as those in North China,.

The 6344 stress data records presented by different methods cover a wide depth in range. Geological and overcoring data provide the near surface information. Borehole breakouts and hydraulic fracturing provide stress indicators down to a depth of 6 km. Focal mechanisms provide stress information throughout the brittle crust down to a depth of 40 km. The tectonic stress regime (Zoback, 1992) could be assigned for 77% of the 6344 A-C quality data records (Table 2), and it is clear that each stress regime constitutes a comparable proportion. This indicates that there is no dominant tectonism of a certain stress regime that could control the stress regime for the majority of China, and thus represents the diversity and complexity of the stress field in China and its adjacent areas to some extent.

4. Continental scale stress pattern

The WSM has revealed that the continental scale stress pattern exists in many plates, and it is controlled primarily by the plate boundary forces. Knowledge regarding the continental scale stress pattern in China and its adjacent area is quite helpful for the analysis of the geodynamic background and how it controls the stress field. Additionally, it is also a prerequisite to identify and investigate the local anomalies or perturbations of the stress field.

Since the FSR-smoothing-method described by Müller et al. (2003) is suitable for identifying a major feature on a certain scale, we adopted this method with a constant search radius of 500 km for the analysis of the continental scale stress pattern.

The smoothing parameter λ was set at 2, and different weight factors were given to different data qualities, namely, 1 for A, 0.75 for B, and 0.5 for C quality. The distance weight was calculated using a tri-cube weight function, and finally determined through the normalization of the weight function by the number of neighbors, n_n, within the search radius (Müller et al., 2003; Wehrle, 1998).

By applying the smoothing method with the parameters mentioned above to the 6344 stress data points with the A-C qualities, we obtained the continental scale variation of the S_{Hmax} orientation for China and its adjacent areas (Fig. 4). The smoothing result clearly reveals that the stress field has a fan-shaped pattern. The S_{Hmax} orientation in China has a clockwise rotation around the boundary of the Indian-Eurasian plate collision, which varies from northwest in the Hindu Kush-Pamir region, to north-south, northeast, east-west, and finally southeast in South China. This feature of stress field rotation is especially obvious at the two tectonic knots of the Indian-Eurasian collision, which are the Himalayan west tectonic knot and the Himalayan east tectonic knot.

By combining Figures 2 and 4, we identified some interesting phenomena for the S_{Hmax} orientations around the different plate boundaries. Around the continental plate boundaries, including the Indian-Eurasian plate collision boundary and the North American plate boundary near Northeast China, S_{Hmax} orientations are often almost perpendicular to the strikes of boundaries, whether from the original stress data or from the smoothing result. However, around the oceanic boundaries, including the

Pacific plate boundary and the Philippine plate boundary, S_{Hmax} orientations appear to be more complex. Some stress data depict the S_{Hmax} orientations to be almost perpendicular to the boundary strikes, but some other orientations are sub-parallel. The smoothing result indicates that S_{Hmax} orientations seem to be sub-parallel to the boundary strikes around the section of the Philippine plate boundary from Taiwan to Japan, and around the majority of the Pacific plate boundary, while around the section of the Philippine plate boundary from Taiwan to the Philippines, the S_{Hmax} orientations are almost perpendicular to the boundary strikes.

In the intermediate regions, the smoothed S_{Hmax} orientations on the continental scale change gradually from those around different plate boundaries. Therefore, it could be deduced that the continental scale stress pattern in China and its adjacent areas is mainly controlled by the surrounding plate boundary forces, which are the Indian-Eurasian plate collision in the western part, and the Pacific plate subduction and the push from the Philippine plate in the eastern part. Since the rotation feature around the Indian-Eurasian plate collision boundary covers the majority of the Chinese mainland, it is reasonable to determine that the boundary force of the Indian-Eurasian plate collision has a larger influence on the continental scale feature of the stress pattern.

This continental scale variation supports the viewpoint that the plate boundary forces are the main factor that controls the first-order stress pattern (Heidbach et al., 2010, 2007; Coblentz et al, 1998; Richardson, 1992; Zoback, 1992). The clockwise rotation of the S_{Hmax} orientation in China from the west to the east coincide with the previous findings (Xie et al., 2015, 2007, 2004; Cui et al., 2005; Xu et al., 2001, 1989; Wang et al., 1993, 1980; Yan et al., 1979; Deng and Zhang, 1979), but this is more distinct in our results. The vast extent of the rotation feature around the Indian-Eurasian plate collision boundary also provides practical stress data evidence for the inference from geodynamic simulations, which means that the Indian-Eurasian collision has the most vital role for the stress pattern in China and its adjacent areas (Zhu et al., 2006; Wang et al., 1996).

5. Local scale stress variability

In addition to the continental scale analysis, a further investigation of local scale stress anomalies and perturbations was conducted. The research regarding local scale variation has also been conducted since the initial study of the WSM (Zoback et al., 1992). A smoothing method with a varying search radius could provide an insight to the inhomogeneity scale of stress orientations (Heidbach et al. 2010) by judging the orientation data spreading within the search radius. This smoothing method has been adopted in the analysis work of the global stress field (Heidbach et al., 2010) and of the stress field in Canada (Reiter et al., 2014). In this method, the mean S_{Hmax} orientation is an important indicator that is used to represent the maximum compressive direction, while the stress wavelength is also a valuable parameter which could partly reflect the spatial inhomogeneity scale of the stress field in a region. This makes the method effective for investigating local stress inhomogeneity. In this study, we use this smoothing method with some adjustments to analyze the inhomogeneity on the local scale of the S_{Hmax} orientation in China and its adjacent areas.

5.1 Adjusted smoothing algorithm

Similar to the method of Heibach et al. (2010), the distance weight was also taken into account in this study. However, it is considered only in the mean S_{Hmax} orientation, but not in the standard deviation (SD) for inhomogeneity scale judgement. The inhomogeneity scale in this study has a specific meaning of describing the horizontal scale of inhomogeneity for the regional stress pattern, and it is not exactly the same as the stress wavelength described by Heidbach et al (2010). In this horizontal scale around one point, the S_{Hmax} orientations could be considered homogeneous, or in other words, the mean S_{Hmax} orientation could represent the regional S_{Hmax} orientations. Conversely, out of this scale, the mean S_{Hmax} orientation is incapable of representing the regional S_{Hmax} orientations. This inhomogeneity scale is determined by the SD of the stress orientations. In case the orientations far from one point are quite different from the uniform orientations in the central region, the stress pattern should not be considered homogeneous for this whole region. However, if the distance weight is still used in the SD calculation, the contribution to SD from these far and disparate orientations would be negligible, and the SD would still be quite small. In this case, the stress pattern of the vast region probably would be indicated as homogeneous by the small value of SD, and the inhomogeneity scale would be a larger value than what it truly represents. Thus, we removed the distance weight factor from the SD calculation when judging inhomogeneity scale.

In addition, data density weight was introduced for the practical stress data distribution. There are a few places where a quantity of disperse orientation data points cluster in a very small region or even at almost the same location (see Figure 2). In this case, no matter how consistent other orientations are, the SD around the disperse cluster would result in a larger scatter, owing to the excessive influence of this cluster in the SD calculation. This SD result comprises a large portion from the uncertainty of the cluster point, which could come from a variation with depth, measurement outliers or other reasons. However, as for the horizontal inhomogeneity, it is the difference among different locations, but not the uncertainty at one location, should be emphasized. Therefore, this SD result cannot reflect the inhomogeneity of the orientation data. To reduce the influence of this factor, we adjusted the weight of the stress data in a cluster by dividing each data entry by the number of neighboring data points within a small distance (assumed to be 1 km in this study). This distance value is equal to 1/50 of the minimum search radius; hence the orientations within this distance can be seen as attached to the same location.

The quality weights were set as 1 for A, 0.75 for B, and 0.5 for C quality, which also match the continental smoothing above. Other settings are the same as those in Heidbach et al.(2010). Distance weighting $w_D = 1/D$ ($D = 25$ km when $D < 25$ km) is applied, where D is the distance from the measured location to the grid point. The criterion for consistency is also the standard deviation of orientations SD≤25°. The lower limit of the data records is n ≥ 5, where n is the number of reliable data records within the search radius. Starting with a search radius of 50 km around each grid point, the radius is increased stepwise by 50 km up to 200 km, then stepwise by 100 km up to 1000 km. The inhomogeneity scale equals the largest radius (r_{max}), which fulfils all criteria (SD ≤ 25°, n ≥ 5), and all the data points within r_{max} around the grid point are used to calculate the mean S_{Hmax} orientation (Reiter et al., 2014; Heidbach et al., 2010). The mean S_{Hmax} orientations are plotted based on the 0.5° grid, and inhomogeneity scales are color coded based on a 0.5 × 0.5° grid in order to display the inhomogeneity of the S_{Hmax} orientation in China and its adjacent areas.

5.2 Mean stress orientations and inhomogeneity scales

By applying the adjusted smoothing method with a varying search radius to the 6344 stress data points with A-C qualities, we obtained the mean S_{Hmax} orientations and inhomogeneity scales for China and its adjacent areas (Fig. 5). Even though there are some places where the stress data are insufficient to obtain reliable results, as shown in the gray areas in Fig. 5, it is still evident that the stress pattern in China and its adjacent areas seems quite inhomogeneous. Compared to the continental scale smoothing map in Fig. 4, the S_{Hmax} orientations in Fig. 5 show the same trend of clockwise rotation from the west to the east, and they also have different behaviors around continental and oceanic boundaries.

Other than the similar features, Fig. 5 exhibits more details and the inhomogeneity scale distribution of S_{Hmax} orientations. In some regions, including regions I, II and III, the S_{Hmax} orientations show more complex variations on local scales than the continental scale orientations. The small inhomogeneity scales in regions I, II and III indicate the strong inhomogeneity for the stress pattern, while regions IV and V have quite large inhomogeneity scales, which indicate the relative homogeneity of their stress patterns.

Regions I and II are located around the two tectonic knots of the Indian-Eurasian collision, and region III can be identified as the tectonic knot of the Philippine plate subduction. Due to the tectonic knot effect, these three regions have extremely inhomogeneous stress fields. Furthermore, this strong inhomogeneity of the stress field results in an intense topographic variation and a complex active fault system (Fig. 1), and makes them the three regions with strongest tectonic movement and seismicity in China and its adjacent areas, namely, the Hindu Kush-Pamir region, South-North seismic zone, and the Taiwan region. The intense topographic variation in concert with the complex active fault system, in turn, enhances the inhomogeneity of the stress pattern to some extent.

In contrast, region IV is located in Northeast China and is separated by part of the North American plate. Region IV is considerably far from the force source of the Pacific plate subduction. The tectonic effect from the North American plate is marginal, and both the North American plate boundary and the Pacific plate boundary near Northeast China are quite flat. These factors from the plate boundary forces make region IV liable to have a more homogeneous stress pattern on the first order. In addition, region IV has very gentle topography and weak faulting, and this could be seen as the second-order mechanism for the homogeneous stress pattern in this region.

Region V is located in the central part of the Tibetan plateau. It is not very far from the Indian-Eurasian collision boundary – although, since the boundary line nearby is quite flat, the plate boundary forces are still relatively simple here. Similar to Northeast China, the central part of the Tibetan plateau also has gentle topography and relatively weak faulting, and these two factors, together with the simple plate boundary forces, make region V another region with a relatively homogenous stress pattern.

The plate boundary forces, as the first-order mechanism, control the macro features of the stress pattern in China and its adjacent areas. Different intensities of the topographic variation and faulting were considered to be the second or third-order mechanisms (Heidbach et al., 2010, 2007; Coblentz et al, 1998; Richardson, 1992; Zoback, 1992), resulting in local variations that cause different inhomogeneity scales of the stress pattern in China and its adjacent areas.

5.3 Further Comparison between regions with inhomogeneous stress patterns

Regions I, II and III seem to have a similar geodynamic interpretation for the strong inhomogeneity of stress pattern, including the effects of the tectonic knot, intense topographic variation and strong faulting activity. When examining these three regions more closely, however, we find some differences. Taiwan (region III) lies right on the tectonic knot of the Philippine plate, the Hindu Kush-Pamir region

(region II) extends approximately 500 kilometers from the Himalayan west tectonic knot, while the South-North seismic zone (region I) extends a quite long distance (over 1500 km) from the Himalayan east tectonic knot. Due to the significant increasing in the distance from tectonic knot, it is reasonable to suggest that the influence of the tectonic knot effect on stress inhomogeneity decreases successively from regions III to region II to region I. This vast inhomogeneity in region I could not be mostly explained by the tectonic knot effect. As revealed above and in previous findings, the stress pattern in and around China is mainly influenced by the Indian-Eurasian collision in the west and by the Pacific plate subduction and the push from the Philippine plate in the east. In this condition, this vast inhomogeneity suggests that the South-North seismic zone (region I) is the separation zone for the western and eastern parts. The effects on different directions from the western and eastern plate boundary forces are comparable, which makes the stress orientation labile here. This interaction between the western and eastern boundary forces is possibly the correct geodynamic interpretation for the vast inhomogeneity of the stress pattern from the point of plate boundary force in this region.

6. Discussion

Both the smoothing results on the continental and local scales have stress orientations with different behaviors around various types of plate boundaries. Generally, S_{Hmax} orientations are almost perpendicular to the strikes around the continental plate boundaries, but they are more complex around the oceanic plate boundaries. Stress data with perpendicular or sub-parallel orientations co-exist, and the smoothing results can also vary around different oceanic plate boundaries. This complexity of stress orientations around oceanic plate boundaries is possibly due to the different tectonic positions in the complex subduction system, such as island arcs, trenches and back-arc basins. More specific studies on the stress environment around subduction zones could help reveal and interpret these complicating factors. One possible and incomplete cause for the continental and oceanic difference is the different mechanical strength of the structure (Tingay et al., 2006). Tingay et al. (2006) suggested that the S_{Hmax} orientation would be generally deflected sub-parallel to mechanically 'weak' structures, but then could be deflected perpendicular to mechanically 'stiff' structures. Compared to a continental plate boundary, there could be more liquid around an oceanic plate boundary to lubricate the boundary and to make it mechanically 'weak'. However, since the subduction surface is three-dimensional, paralleling the strike is not the only choice for paralleling the subduction structure. Therefore, this cause does not totally explain the difference. More specific and further studies on this difference are worthwhile and they could be significant for identifying and explaining the different behaviors and mechanisms for the stress pattern between continental and oceanic plate boundaries.

The stress data integration provides a decent dataset, but in some regions in China, there are still few focal mechanism data points and also few stress measurement data points. Consequently, it is difficult to obtain more details about the stress environment in the regions lacking data. Adopting seismic data of small earthquakes as well as carrying out more stress measurements would be useful and meaningful to contribute to stress orientation data.

7. Conclusions

In this study, we attempted to integrate stress data and analyze the crustal stress patterns for China and its adjacent areas. For the stress data integration, a total of 6089 raw stress data records from the latest China Stress Database were ranked and standardized according to the latest criteria of the World Stress Map. The resulting 5643 stress data records were integrated into the 2016 WSM release. The enriched database provides a solid basis for the crustal stress analysis of China and its adjacent areas.

As for the crustal stress pattern analysis, with the 6344 stress data records with A-C qualities from the integrated dataset (2016 WSM release), the patterns of stress orientation on the continental and local scales, were analyzed using different smoothing algorithms. The S_{Hmax} orientation in China rotates clockwise from the west to the east, resulting in a fan-shaped crustal stress pattern on the continental scale. The inhomogeneity scale distribution indicates that Northeast China and the central part of the Tibetan plateau have large scale stress patterns, while the South-North seismic zone, the Hindu Kush-Pamir region, and the Taiwan region have small scale stress patterns in China and its adjacent areas. The results are interpreted from different orders. The plate boundary forces are the first-order factors, and control the macro features of the crustal stress pattern. The second-order mechanism comes from topographic variation and faulting activity, and these factors lead to local variations of the stress pattern. The vast inhomogeneity of the stress pattern around the South-North seismic zone supports a separation zone for the western and eastern boundary forces around China.

Acknowledgments

This work was supported jointly by the Institute of Crustal Dynamics, China Earthquake Administration Research Fund [grant number ZDJ 2014-14 and ZDJ2015-06], National Science and Technology Support Program [grant number WSFD-07] and SinoProbe-06-04. We thank all the scholars for providing the stress data records, and we thank R. Yao for the assistance in the stress data collection. The maps were generated through CASMI (Heidbach et al., 2007) and GMT software (Wessel et al., 2013). We are also grateful to the reviewers for their constructive comments and suggestions.

References

Balfour, N.J., Cassidy, J.F., Dosso, S.E., Mazzotti, S., 2011. Mapping crustal stress and strain in southwest British Columbia. Journal of Geophysical Research, 116 (B3), 428-452

Bird, P., Li, Y., 1996. Interpolation of principal stress directions by nonparametric statistics: global maps with confidence limits. Journal of Geophysical Research, 101 (B3), 5435-5443.

Bird, P., Ben-Avraham, Z., Schubert, G., Andreoli, M., Viola, G., 2006. Patterns of stress and strain-rate in southern Africa. Journal of Geophysical Research, 111 (B8), 139-149.

Brudy, M., Kjørholt, H., 2001. Stress orientation on the Norwegian continental shelf derived from borehole failures observed in high-resolution borehole imaging logs. Tectonophysics, 337 (1-2), 65-84.

Coblentz, D., Richardson, R.M., 1995. Statistical trends in the intraplate stress field. Journal of Geophysical Research, 100 (B10), 20245-20255.

Coblentz, D., Zhou, S., Hillis, R.R., Richardson, R.M., Sandiford, M., 1998. Topography, boundary forces, and the Indo-Australian intraplate stress field. Journal of Geophysical Research, 103 (B1), 919-931.

Camelbeeck, T., de Viron, O., Van Camp,M., Kusters, D., 2013. Local stress sources inWestern Europe lithosphere from geoid anomalies. Lithosphere, 5 (3), 235-246.

Cui, X. F., Xie, F. R., Zhao, J. T., 2005. The regional characteristics of focal mechanism solutions in China and its adjacent areas. Seismology and Geology, 27 (2), 298-307.

Davis, J. C., 1986. Statistics and Data Analysis in Geology, 2nd ed., 646 pp. John Wiley, New York.

Deng, Q. D. (Chief Editor), 2007. Map of Active tectonics in China. Beijing: Seismological Press.

Deng, Q. D., Zhang, Y. M., 1979. On the tectonic stress field in china and its relation to plate movement. Physics of the Earth and Planetary Interiors, 18(4), 257-273.

Fan, T. Y., Long, C. X., Yang, Z. Y., Chen, Q. C., Wu, Z. H., Shao, Z. G., Tong, Y. B., 2012. Comprehensive modeling on the present crustal stress of China mainland with the viscoelastic spherical shell. Chinese Journal of Geophysics, 55(4), 1249-1260.

Fuchs, K., Muller, B., 2001. World Stress Map of the Earth: a key to tectonic processes and technological applications. Naturwissenschaften, 88(9), 357-371.

Hansen, K.M., Mount, V.S., 1990. Smoothing and extrapolation of crustal stress orientation measurements. Journal of Geophysical Research, 95 (B2), 1155-1165.

Hardebeck, J.L., Michael, A., 2004. Stress orientations at intermediate angels to the San Andreas Fault, California. Journal of Geophysical Research, 109 (B11), 285-296.

Heidbach, O., Reinecker, J., Tingay, M.R.,Müller, B., Sperner, B., Fuchs, K.,Wenzel, F., 2007. Plate boundary forces are not enough: second and third-order stress patterns highlighted in the world stress map database. Tectonics, 26(6), 438-451.

Heidbach, O., Höhne, J., 2008. CASMI — A visualization tool for the World Stress Map database. Computer and Geosciences, 34: 783-791

Heidbach, O., Tingay, M., Barth, A., Reinecker, J., Kurfeß, D., Müller, B., 2008. The World Stress Map database release. doi:10.1594/GFZ.WSM.Rel2008.

Heidbach, O., Tingay,M., Barth, A., Reinecker, J., Kurfeß, D. and Müller, B., 2009. The World Stress Map based on the database release 2008, equatorial scale 1:46,000,000, Commission for the Geological Map of the World, Paris. doi:10.1594/GFZ.WSM. Map2009.

Heidbach, O., Tingay, M.R.P., Barth, A., Reinecker, J., Kurfeß, D., Müller, B., 2010. Global crustal stress pattern based on the World Stress Map database release 2008. Tectonophysics, 482 (1-4), 3-15.

Heidbach, O., Rajabi, M., Reiter, K., Ziegler, M., WSM Team (2016): World Stress Map Database Release 2016. GFZ Data Services, doi:10.5880/WSM.2016.001.

Hillis, R. R., Meyer, J. J., Reynolds, S. D., 1998. The Australian stress map. Journal of the Geological Society, 29(4), 420-427.

Hodges, J.L., Lehmann, E.L., 1967. On medians and quasi medians. Journal of the American Statistical Association, 62 (319), 926-931.

Lund, B. and Townend, J., 2007. Calculating horizontal stress orientations with full or partial knowledge of the tectonic stress tensor. Geophysical Journal International, 170, 1328-1335.

Mardia, K.V., 1972. Statistics of Directional Data: Probability and Mathematical Statistics. Academic Press, London. 357 pp.

Müller, B., Zoback, M.L., Fuchs, K., Mastin, L., Gregersen, S., Pavoni, N., Stephansson, O., Ljunggren, C., 1992. Regional patterns of tectonic stress in Europe. Journal of Geophysical Research, 971(B8), 11783-11803

Müller, B., Wehrle, V., Zeyen, H.J., Fuchs, K., 1997. Short-scale variations of tectonic regimes in the western European stress province north of the Alps and Pyrenees. Tectonophysics, 275, 199-219.

Müller, B.,Wehrle, V., Hettel, S., Sperner, B., Fuchs, K., 2003. A new method for smoothing orientated data and its application to stress data. Geological Society

London Special Publications, 209 (1), 107-126.

Ratanaruamkarn, S., Niewiadomska-Bugaj, M., Wang, J.-C., 2009. A new estimator of a circular median. Communication in Statistics- Simulation and Computation, 38 (6), 1269-1291.

Rajabi, M., Tingay, M., Heidbach, O., 2016. The present-day stress field of New South Wales, Australia. Australian Journal of Earth Sciences, 63, doi: 10.1080/08120099.0812.2016.01135821, 1-21.

Rebaï, S., Philip, H., Taboada, A., 2007. Modern tectonic stress field in the mediterranean region: evidence for variation in stress directions at different scales. Geophysical Journal International, 110(1), 106-140.

Reinecker, J., Tingay, M., Müller, B., Heidbach, O., 2010. Present-day stress orientation in the molasse Basin. Tectonophysics, 482 (1), 129-138.

Reiter, K., Heidbach, O., Schmitt, D., Haug, K., Ziegler, M., Moeck, I., 2014. A revised crustal stress orientation database for Canada. Tectonophysics, 636, 111-124.

Richardson, R.M., Reding, L.M., 1991. North American plate dynamics. Journal of Geophysical Research, 96 (B7), 12201-12223.

Richardson, R.M., 1992. Ridge forces, absolute plate motions, and the intraplate stress field. Journal of Geophysical Research, 97, 11739-11748.

Sbar, M.L., Sykes, L.R., 1973. Contemporary compressive stress and seismicity in eastern North America, an example of intraplate tectonics. Geological Society of America Bulletin, 84, 1861-1881.

Schmitt, D.R., Currie, C.A., Zhang, L., 2012. Crustal stress determination from boreholes and rock cores: Fundamental principles. Tectonophysics, 580, 1-26.

Sperner, B., Müller, B., Heidbach, O., Delvaux, D., Reinecker, J., Fuchs, K., 2003. Tectonic stress in the earth's crust: advances in the world stress map project. Geological Society London Special Publications, 212(1), 101-116.

Stephansson, O., Zang, A. (2012): ISRM suggested methods for rock stress estimation - Part 5: Establishing a model for the in-situ stress at a given site. Rock Mechanics and Rock Engineering, 45(6), 955-969.

Tingay, M., Muller, B., Reinecker, J., Heidbach, O., 2006. State and origin of the present-day stress field in sedimentary basins: New results from the World Stress Map Project. In The 41st U.S. Symposium on Rock Mechanics (USRMS). Golden, CO: American Rock Mechanics Association.

Townend, J., Zoback, M.D., 2004. Regional tectonic stress near the San Andreas fault in central and southern California, Geophysical Research Letters, 31, L15S11, doi:10.1029/2003GL018918.

Townend, J. 2006. What do Faults Feel? Observational Constraints on the Stresses Acting on Seismogenic Faults, Earthquakes: Radiated Energy and the Physics of Faulting, Geophysical Monograph Series 170, 313-327.

Townend, J., Zoback, M.D., 2006. Stress, strain, and mountain building in central Japan, Journal of Geophysical Research, 111, B03411, doi:10.1029/2005JB003759.

Wang, S. Y., Chen, P. S., 1980. A numerical simulation of the present tectonic stress field of china and its vicinity. Chinese Journal of Geophysics, 23(1), 35-45.

Wang, S. Y., Gao, A. J., Xu, Z. H., 1993. The characteristics of focal mechanism solution in China and its adjacent areas. China earthquake zoning corpus. Earthquake Defense Department, China Earthquake Administration, Beijing: Seismological Press, 10-26.

Wang, S. Y., Xu, Z. H., Yu, Y. X., 1996. Inversion for the plate driving forces acting at the boundaries of China and its surroundings. Chinese Journal of Geophysics, 39(6), 764-771.

Watson, G. S., 1985. Interpolation and smoothing of directed and undirected line data. In: Krishnajah, P. R. (Editor), Multivariate Analysis-VI. Elsevier Science, New York, pp. 613-625.

Wehrle, V., 1998. Analytische Untersuchung intralithosphärischer Deformationen und Numerische Bestimmung krustaler Spannungsdomänen, TH Karlsruhe, Karlsruhe, 167 pp.

Wessel, P., Smith,W.H.F., Scharroo, R., Luis, J.,Wobbe, F., 2013. Generic mapping tools: improved version released. Eos Transactions American Geophysical Union, 94(45), 409-410.

Xie, F. R., Cui, X. F., Zhao, J. T., Chen, Q. C., Li, H., 2004. Regional division of the recent tectonic stress field in china and adjacent areas. Chinese Journal of Geophysics, 47(4), 745-754.

Xie, F. R., Chen, Q. C., Cui, X. F., Li, H., Yang, S. X., Guo, Q. L., Chen, L. W., Xu, Z. H., Zhang, Y. S., Dou, S. Q., Zhao, J. T., Zhang, Z. S., Liu, C. Y., Wang, G. J.,

2007. Fundamental database of crustal stress environment in continental China. Progress in Geophysics, 22 (1), 131-136.

Xie, F. R. (Chief Editor), 2015. Recent tectonic stress map of China and its adjacent areas. Jiangsu: Sinomaps Press.

Xu, Z. H., Wang, S. Y., Huang, Y. R., Gao, A. J., 1989. The tectonic stress field of Chinese continent deduced from a great number of earthquake. Chinese Journal of Geophysics, 32(6), 636-647.

Xu, Z. H., 2001. A present-day tectonic stress map for eastern Asia region. Acta Seismologica Sinica, 14(5), 524-533.

Yan, J. Q., Shi, Z. L., Wang, S. Y., Huan, W. L., 1979. Some Features of the recent tectonic stress field of China and Environs. Acta Seismologica Sinica, 1 (1), 9-24.

Zang, A., Stephansson, O., 2010. Stress Field of the Earth's Crust. Springer, Netherlands, Dordrecht.

Zhang, P. Z., Wang, Q., Ma, Z. J., 2002. GPS velocity field and active crustal blocks of contemporary tectonic deformation in continental China. Earth Science Frontiers, 9 (2), 430-441

Zhu, S. B., Shi, Y. L., 2006. Study the controls of the tectonic stress of China mainland. Science in China Series D: Earth Sciences, 36(12), 1077-1083

Zoback, M.L., Zoback, M.D., Adams, J., Assumpção, M., Bell, S., Bergman, E.A., Blümling, P., Brereton, N.R., Denham, D., Ding, J., Fuchs, K., Gay, N., Gregersen, S., Gupta, H.K., Gvishiani, A., Jacob,K., Klein, R., Knoll, P.,Magee,M.,Mercier, J.L.,Müller, B.C., Paquin,C., Rajendran, K., Stephansson, O., Suarez, G., Suter, M., Udías, A., Xu, Z.H., Zhizhin, M., 1989. Global patterns of tectonic stress. Nature, 341, 291-298.

Zoback, M.L., 1992. First and second order patterns of stress in the lithosphere: the World Stress Map project. Journal of Geophysical Research, 97, 11703-11728.

Fig. 1. The tectonic background of China and its adjacent areas. The topography (SRTM15 PLUS) is color coded. The gray lines are the active faults (Deng, 2007). The blue fault lines indicate the main plate boundaries around China (Xie et al., 2015). The red arrows indicate the plate motion direction relative to the Eurasian Plate (Xie et al., 2015).

Table 1. *Type and quality of the* S_{Hmax} *orientation data in China and its adjacent areas (latitude 0-60°N, longitude 45°-155°E).*

Fig. 2 Stress map in China and its adjacent areas of the 6,344 stress data records with A–C qualities excluding Possible Plate Boundary Events (PBEs). The bars represent the orientations of maximum horizontal compressional stress S_{Hmax}, and the bar length is proportional to quality. The colors indicate the stress regimes with red representing normal faulting (NF), green representing strike-slip faulting (SS), blue representing thrust faulting (TF), and black representing an unknown regime (U).

Fig. 3 Comparison between the WSM database release2008 and 2016 in China and its adjacent areas. Fig. 3a) Stress data with A-C qualities excluding PBEs in WSM database release 2008; Fig. 3b) Only new stress data with A-C qualities excluding PBEs in WSM database release 2016. The symbols are the same as in Fig. 2.

Table 2. *Statistics of stress regime for 6344 A-C quality stress data in China and its adjacent areas*

Fig. 4 Smoothed S_{Hmax} orientations on the continental scale and indicators of stress field rotation in China and its adjacent areas. The thin red bars indicate the smoothed S_{Hmax} orientations on the continental scale using a quality- and distance-weighted algorithm (Müller et al., 2003). The search radius is r = 500 km, a minimum number of neighbors $n_{min} = 5$, a minimum value of the sum of quality weight factors of the nearest neighbors $s_q = 5$, and a minimum for the sum of the weight terms of the nearest neighbors $s_w = 1$, within the search radius is requested for calculating the mean stress orientation at a grid point. The solid red dotted bars represent the macro feature of the smoothing result of the S_{Hmax} orientation in China. The blue fault lines indicate the main plate boundary around China (Xie et al., 2015).

Fig. 5 Mean S_{Hmax} orientations and inhomogeneity scales in China and its adjacent areas. The mean S_{Hmax} orientations are displayed through the black bars, indicating the S_{Hmax} orientations on a $0.5 \times 0.5°$ grid. The inhomogeneity scales equal to the largest radii r_{max}, which fulfils the confidence criterion ($SD \leqslant 25°$) and the data record criterion ($n \geqslant 5$) are color coded. The gray areas are the areas without reliable results. The blue fault lines indicate the main plate boundary around China (Xie et al., 2015). I~V and white rectangles indicate distinctive regions.

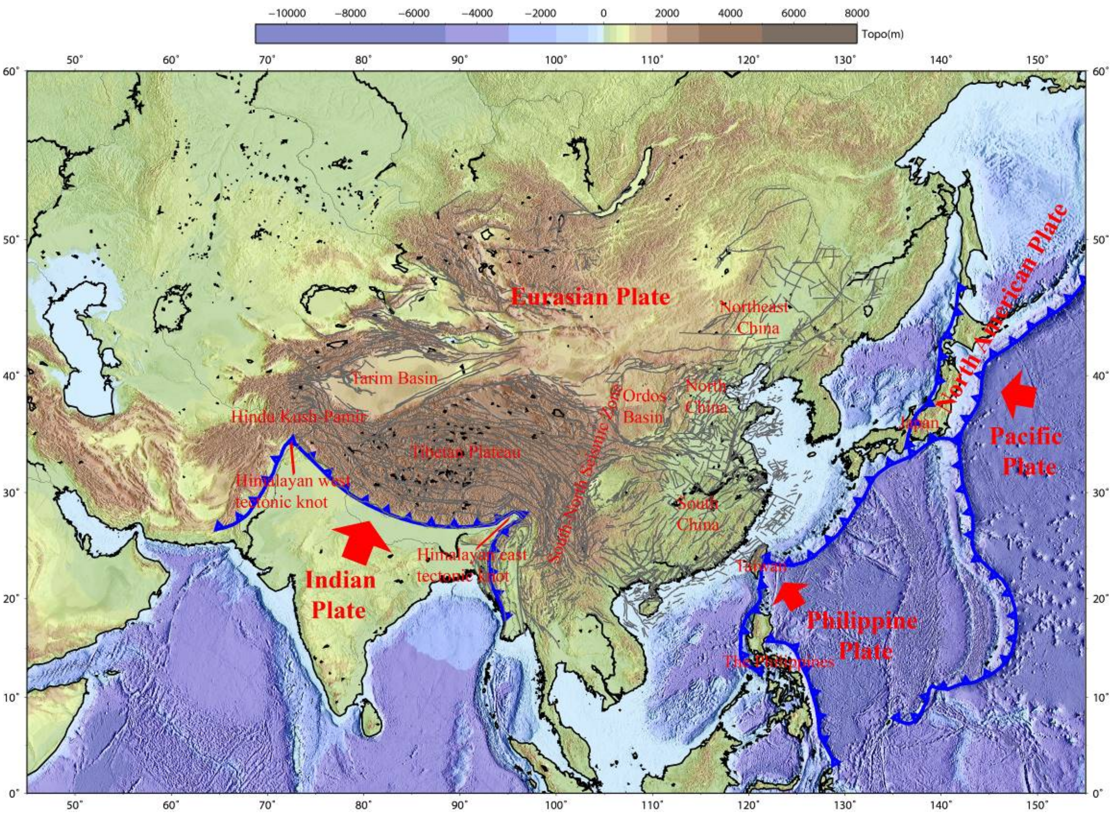

Fig. 1. The tectonic background of China and its adjacent areas.

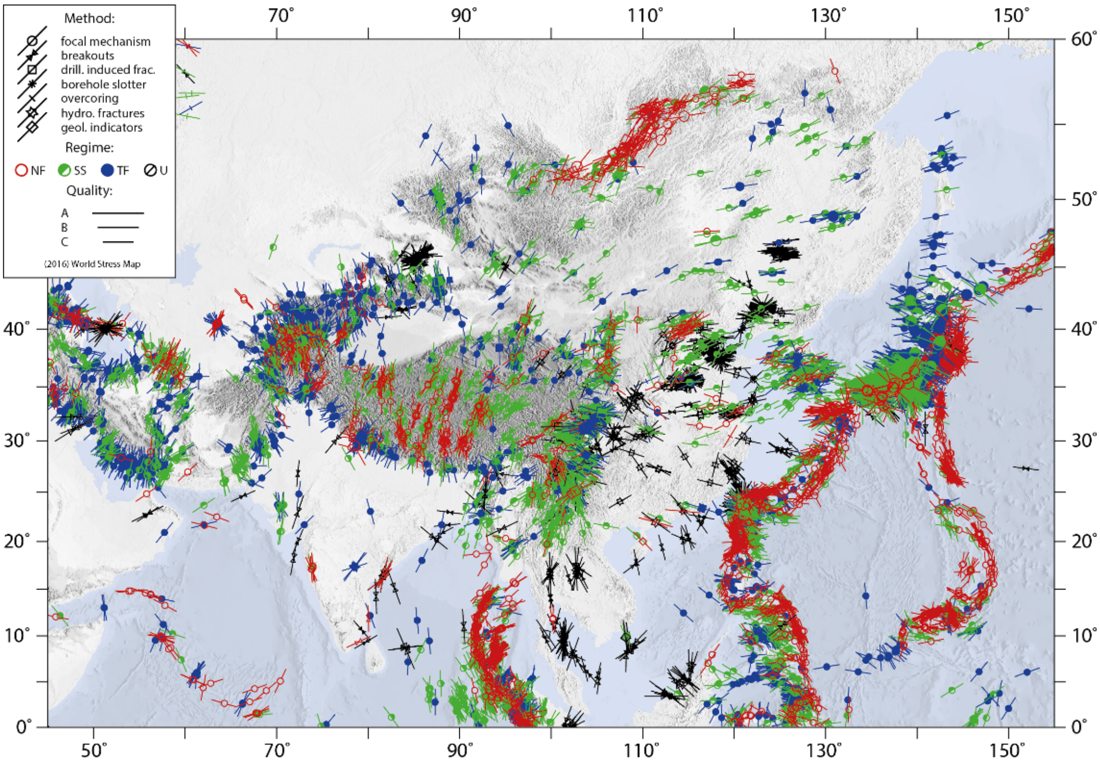

Fig. 2 Stress map in China and its adjacent areas based on the 2016 WSM release using the 6,344 stress data records with A–C qualities excluding Possible Plate Boundary Events (PBEs).

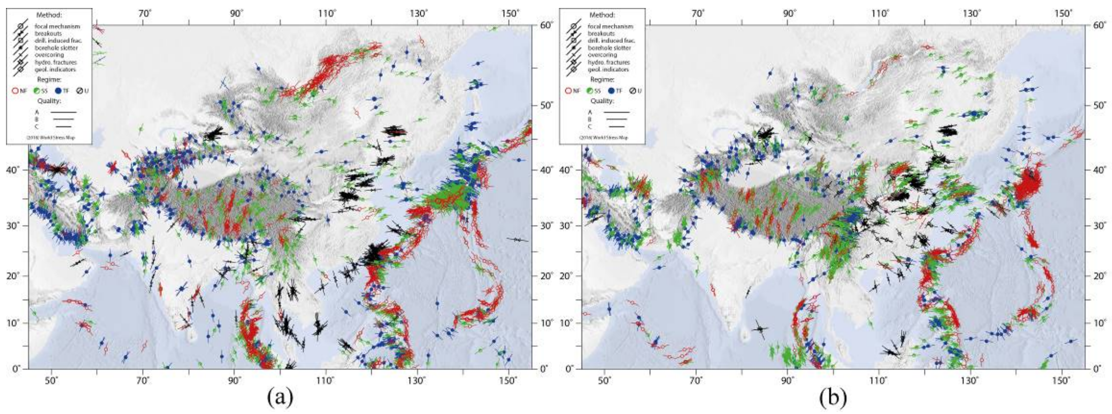

Fig. 3 Comparison between the 2008 WSM release and the 2016 WSM release in China and its adjacent areas.

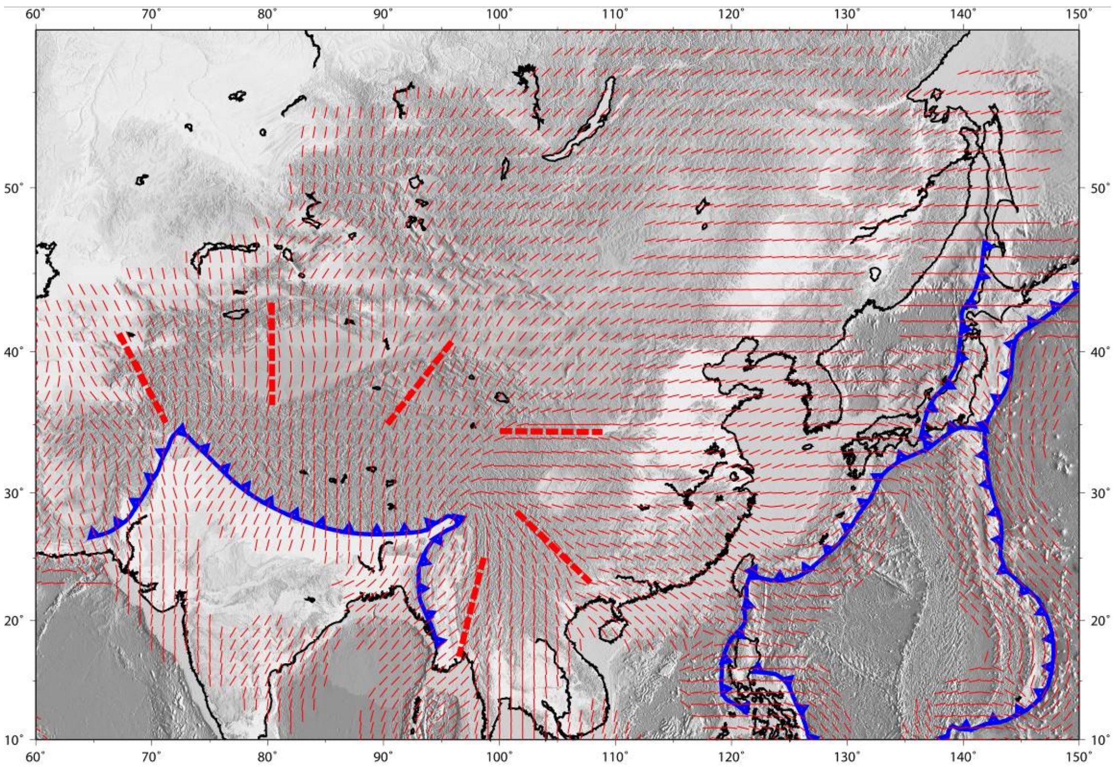

Fig. 4 Smoothed S_{Hmax} orientations on the continental scale and indicators of stress field rotation in China and its adjacent areas.

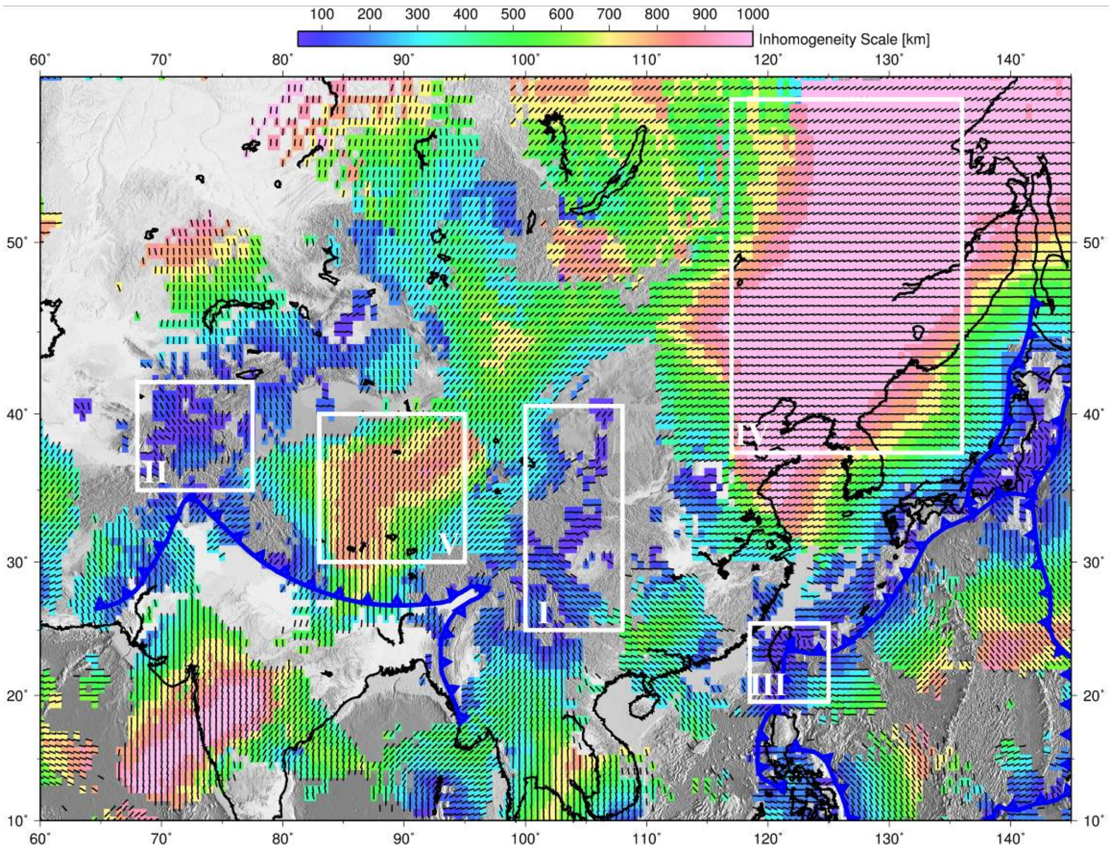

Fig. 5 Mean S_{Hmax} orientations and inhomogeneity scales in China and its adjacent areas.